Environmental Sciences Europe

RESEARCH

Open Access

Improving the forecast of fine dust emission and transmission from cattle barns: a comprehensive data package and analysis

Ehab Mostafa[1*], Jessica Paßmann[2], Hassan R. S. Abdellatif[1] and Wolfgang Buescher[2*]

Abstract

The livestock sector emits harmful gases and bioaerosols, impacting animals, plants, and human health. Ventilation systems in livestock buildings disperse polluted air, affecting nearby air quality depending on the wind patterns and atmospheric stability. Understanding pollutant emission and transmission is crucial for environmental mitigation. This study focuses on fine dust dispersion from dairy cattle buildings. Chemical and microscopic analyses were conducted to identify the cattle barn dust sources. Particle mass emissions were quantified by measuring particle mass concentrations and air volume flow using the tracer gas decay method. Seasonal and daily effects on dust emissions were studied. Remarkably, particle emissions remained below prescribed values in Germany. Additionally, particle transmission, including resuspension and adsorption parameters, was investigated using a developed wind tunnel. Resuspension measurements revealed minimal resuspended particle mass due to low ground wind speeds. Notably, wheat, as a model plant, exhibited high adsorption rates, which increased with particle size. Overall, the findings for resuspension and adsorption parameters provide an initial database for understanding fine dust transmission from cattle barns.

Keywords Fine dust transmission, Particle characterization, Ventilation rate, Resuspension and adsorption parameters

Introduction

Resuspension is an important source of indoor airborne particulate matter (PM) in occupied buildings [6] and therefore contributes to the degradation of air quality in livestock buildings [19]. Airborne bioaerosols can adversely affect the health of both humans and animals, not only within buildings, but also in the surrounding neighborhood [10], including the plants around these buildings [21].

*Correspondence:
Ehab Mostafa
emostafa@agr.cu.edu.eg
Wolfgang Buescher
buescher@uni-bonn.de
[1] Agricultural Engineering Department, Faculty of Agriculture, Cairo University, El-Gammaa Street, Giza 12613, Egypt
[2] Institute of Agricultural Engineering, Faculty of Agriculture, Bonn University, Nussallee 5, 53115 Bonn, Germany

The pollution load with PM impacts plants in an area by inhibiting certain physiological functions, such as photosynthetic pigment degradation, membrane damage, alterations in metabolic functions, and enzyme activities. Additionally, reduced growth rate and yield suppression in crops may occur in response to elevated concentrations of air pollutants. The impact of air pollutants on plant growth and productivity varies depending on the physical and chemical properties of the pollutants [21]. Deposition and accumulation of fine particles on the plant leaves reduces the light penetration and therefore chlorophyll content and photosynthetic rate will decrease. In addition, the stomata opening will be blocked and thus the transpiration rate will decline [3].

Accordingly, animal husbandry systems with improved air quality will be essential in future to protect human and animal health [4]. Animal breeders are always concerned about the issue of PM pollution near animal barns

[7]. Thus, the systems for reducing the dust concentrations in the barns are being intensively studied [5]. Furthermore, measurements of dust emission have been increasingly carried out on animal barns, which improves the predictions for dispersion simulations [1]. To make precise predictions of dust spread, the determination of the emission factors is very important [15, 16]).

In addition, the relevant influencing factors of transmission should be considered in the propagation models [9]. A dispersion simulation for predicting dust transmission and deposition can only deliver realistic results if the particle-specific parameters such as size, shape, and density are taken into account [15, 16]. Dust produced from the agricultural sector is difficult to be described with the models due to its heterogeneous composition [25]. The adsorption behavior of plants should be mentioned in particular, which makes a further contribution to the separation of fine dust from the ambient air [22]. In the environment of barns, the adhesion processes of particles on plants play a decisive role [12].

In this study, a dependency of the particle adhesion on the plants and the wind speed is assumed. The emitted dust from the animal buildings settles mainly on the surrounding areas through resuspension, where the particles are deposited on the surfaces and may get back again into the air volume flow [13]. However, developing models to simulate resuspension processes is very difficult with regard to the resuspension behavior of particles [23].

The objective of this study is to provide a comprehensive data package for improving the reliability and performance of propagation simulations of dust emission and transmission from cattle barns. Specifically, we aim to characterize the particle matters collected from a dairy cow barn during three different seasons and study their aerodynamic properties using a sedimentation cylinder. The dust emissions from the cattle barn will be examined by measuring particle number and particle mass concentrations. The decay method with the tracer gas SF6 will be used to determine the air exchange rate in the barn. Furthermore, a database will be created for the transmission parameters resuspension and adsorption using a developed wind tunnel. The data collected can help to understand and predict the dust flux and the sensitivity of different dust schemes over regions and can also be useful for future research on dust transmission processes and estimation of the deposition loads.

Material and methods

Characterization of the trial barn

The particulate matter (PM) emission measurements were conducted in a natural-ventilated dairy cattle located at Heidgen (50°40′07.65"N 7°01′32.55"E), North Rhine Westphalia, Germany. The dairy cowshed as illustrated in Fig. 1 is an extension to an existing old building with a yard measuring 225 m^2 (25 m length and 9 m width). The old building is still used for feeding and as a waiting room. Preliminary experiments conducted with a smoke generator indicated that there was insufficient airflow into the old building. For this reason, the emission measurements were carried out only in the low-level barn. The barn has a 4.2 m ridge, 2.7 m eave height, and a roof pitch of 20 degrees. The barn has a gross air volume of 776.3 m^3 and an animal volume of 57.9 m^3 for 35 cows. Windbreak nets with an area of 11.4 m^2 are attached to the eaves of the barn at a height of 1.7 m. The barn has a manure pit with a depth of 0.5 m. The ventilation system in the barn is limited to eaves–ridge ventilation. The barn is bedded daily during the evening time with three straw round bales (1.2 m diameter). Concentrate and mineral feed are allocated via the concentrate feed retrieval station. Manure removal, feeding process, and water supply are achieved manually.

Meteorological data

Climate parameters including wind direction (Φ_W), wind speed (v_w), and outside temperature (T_a) were recorded using an ultrasonic anemometer (from METEK Meterelogische Messtechnik GmbH, Germany). The device was installed 0.6 m above the barn ridge. Additionally, indoor temperature and humidity were monitored at 1-min intervals using a sensor (type FHA646R, Ahlborn Mess- und Regelungstechnik GmbH, Germany).

Analysis of collected particles from dairy cattle barn and determination of its geometry

Two analysis methods were employed at the institute of animal nutrition—University of Bonn in Germany to characterize the primary source of cattle dust. First, particles were quantitatively examined using the Weende analysis method [17], traditionally used in feed analysis. This approach provided a detailed overview of both inorganic and organic components in dairy cattle barn dust. Additionally, other cattle dust samples were analyzed using the Euro Elemental Analyzer (Euro Vector company, Italy) to determine the carbon–nitrogen (C:N) ratio. Specifically, two samples were collected: one naturally sedimented sample (S1) and another from the PM sampler described earlier (S2).

On the determination of the geometry of particles, the emissions flow rate can be precisely calculated by determining particle mass concentration and the geometry of particles, which is of utmost importance in the study. In the current study, two dust collection techniques are employed. First, a horizontal PM sampler was modified to enable the collection of larger dust quantities. The modified sampler, depicted in Fig. 2,

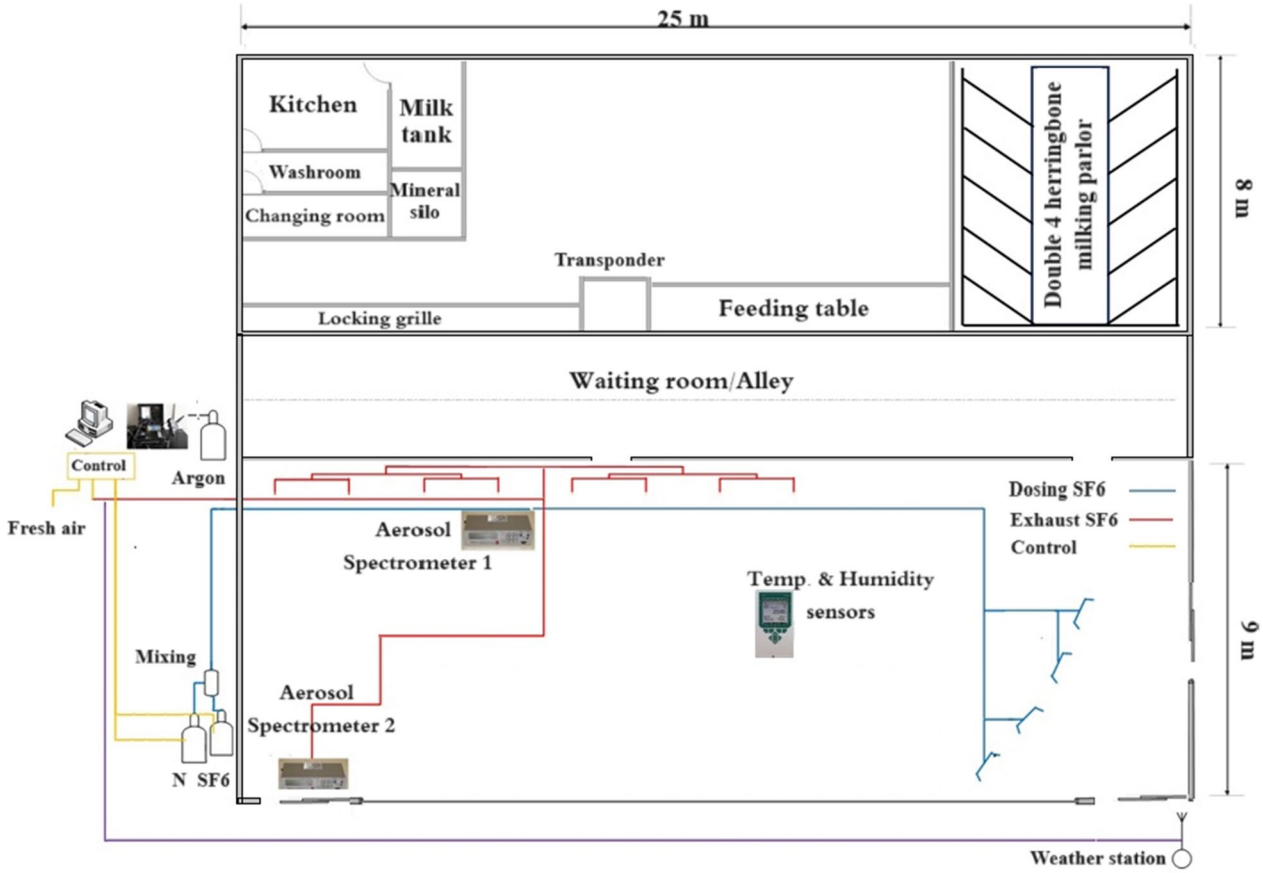

Fig. 1 Schematic diagram of the examined natural-ventilated dairy cattle barn

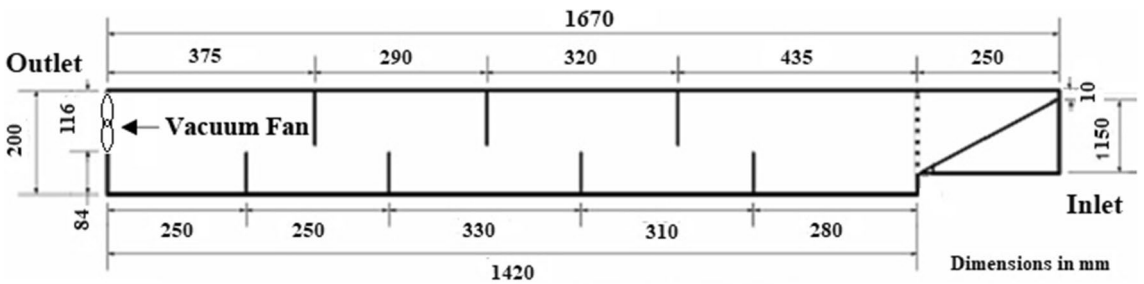

Fig. 2 Scheme for the developed PM sampler (side view)

consisted of a plywood channel measuring 1.67 m in length, 0.2 m in height, and 0.1 m in width. Internally, the sampler was divided into eight boxes, with seven wooden baffle plates alternately mounted at the bottom and top surfaces. Metal containers were strategically placed within these boxes to facilitate easier dust extraction. Additionally, a small vacuum fan (specifically, the Model 4412 FGL from ebm Papst company, Germany) was installed and operated at 1600 rpm with a volume flow of 94 m^3/h. This fan draws air from one side of the sampler, creating a flow through the opposite opening (measuring 0.1 m in width and 0.01 m in height).

Since high humidity in the cattle shed leads to the agglomeration of particles in the sampler, 220 mm wide 3 copper bands heating foil (CANDOR GmbH. Leipzig. Germany) was used to ensure a precise analysis of the physical parameters.

The Andersen Cascade-Impactor collector (Schaefer Company, Langen, Germany) served as the second sampler for particles in the cattle barn. This impactor divides particulate matter (PM) into eight size classes ranging from 0.4 to > 11.0 µm. The air, laden with particles, was drawn above the impactor using a constant air volume flow of 28.3 L/min, facilitated by a connected vacuum pump. Each impactor stage features a unique perforation and was equipped with mounted glass plates. Sampling duration was 20 min.

The collected particles on the glass plates underwent direct analysis using a scanning light microscope (Leitz DMRB Company, Germany). An attached digital camera allowed us to photograph the observed dust particles, subsequently processed using the DISKUS Version 4.30.138 software. For analysis, two different lenses were utilized: a 20× magnification lens for overview images and a 100× magnification lens for detailed shots. The images were evaluated based on particle size, area, circumference, and diameter. The equivalent diameter for each irregularly shaped particle was determined geometrically, considering a sphere with the same geometric property. Finally, the particle size-specific shape factor (κ), particle density (ρ), and PM mass concentration were calculated using the particles collected by the horizontal sampler, following the approach by [15].

Estimating PM emissions from the investigated dairy cattle barn

To estimate dust emissions from the investigated dairy cattle barn, both particle number concentration and air volume flow were measured, following the approach by Mostafa and Buescher [14]. Subsequently, particle mass concentration was calculated based on the particles' shape factor and density, as outlined by Mostafa et al. [15]. By combining the particle mass concentration with the barn's ventilation rate, dust emissions from the dairy cow barn were estimated, consistent with Mostafa and Buescher [14, 15]. The particle concentration measurements were carried out continuously in parallel with the meteorological measurements for four consecutive days during transition (from 17th to 21st April), summer (from 16 to 20th June), and winter (from 14 to 18th January) season to identify the seasonal dependencies.

The particle number concentrations per cubic meter of air were measured using two calibrated aerosol spectrometers (Model 1.108 GRIMM Aerosol techniques, Ainring, Germany). The data were stored at one-minute intervals across 15 different size classes (ranging from 0.3 to > 20.0 µm). To identify measuring points within the barn as illustrated in Fig. 1, a smoke machine was employed to specify the air pattern for maximizing the exposure of the spectrometer to the polluted air. Additionally, the particle mass concentration in the exhaust air was derived from the particle number concentration.

Two gravimetric samplers working with radially symmetrical suction heads were used to measure the mass concentration of particles according to VDI 2463-8 [24]. The gravimetric sampler includes a radially symmetrical suction head, a vacuum pump with an air volume flow of 2.7–2.8 $m^3\ h^{-1}$, a gas flowmeter, an integrated cooling unit, and a fiberglass filter. Constant air humidity using hydrophilic granulate was maintained. Particle mass concentration was calculated by measuring the weight difference of balanced filters before and after sampling, along with the volume of air that passed through.

Measuring the air volume flow

In this study, the air exchange rate was determined using the tracer gas decay method (TGD), following Mostafa et al. [16]. Sulfur hexafluoride (SF6) was selected as the tracer gas due to its low presence in the atmosphere (0.85 to 1.5 ppt). SF6 is chemically inert, biologically odorless, tasteless, non-toxic, and neither flammable nor explosive. Its molar mass of 146.05 kg/mol makes it five times heavier than oxygen (28.96 kg/mol).

Polyethylene (PE) tubes were positioned with an inside diameter of 4 mm, equipped with eight nozzles, at a distance of 0.75 m to create a cascade structure (Fig. 1). To account for SF6's high molar mass, a mixture of SF6 and CO2 was introduced into a mixing container, subsequently supplying the barn's airflow via the dosing unit. Pressure reducer electromagnetic valves, controlled by software, were installed on the gas cylinders. Continuous air sampling occurred using a suction hose system. The Leakmeter 200 (from Meltron Qualitek Messtechnik GmbH, Neuss, Germany) drew air through a 15 L/min volume flow vacuum pump, serving as a leak detection device. SF6 detection utilized an electron capture detector, resulting in a high-resolution decay curve from measurements taken every second (Fig. 3).

The measurement software controls the settling time (120 s), dosing time (150 s), and actual measurement time (700 s). With these settings, approximately 4 air change rates per hour can be determined. During the dosing period, CO_2 and SF6 were dosed into the barn at specific flowrates, while argon acts as a carrier gas for the measuring device. The air sampling of the fresh air takes place on the side of the barn facing away from the wind, both at the beginning and end of each measurement. This is followed by the dosing phase of SF6, during which the SF6 concentration in the exhaust air increases steadily. After completing the phase, the maximum concentration in the barn is reached. The subsequent measurement phase records the time required until the SF6 concentration in the barn has

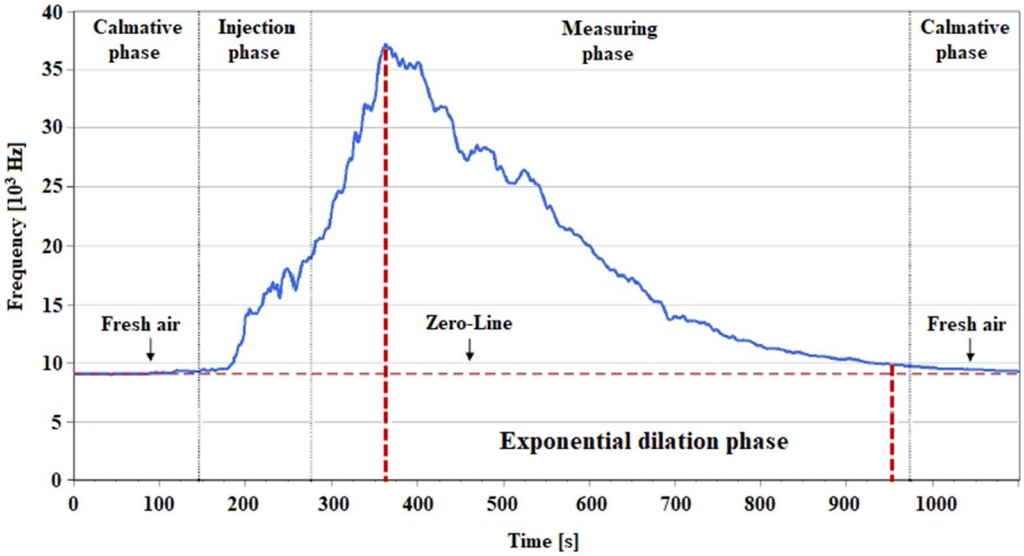

Fig. 3 SF6 measurement phases

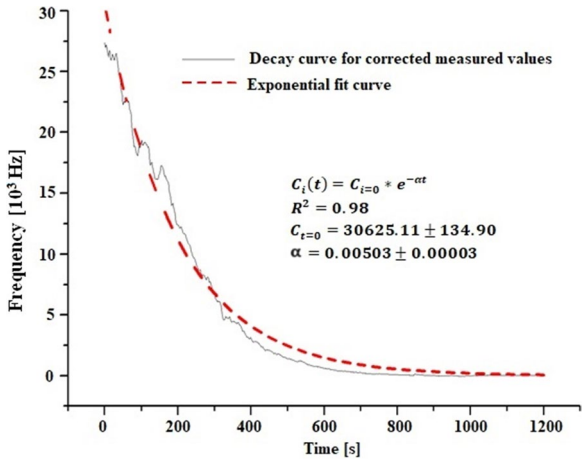

Fig. 4 SF6 tracer gas decay exponential curve

subsided. The presented SF6 measurement is a validated method for determining the air volume flow.

The data were analyzed using Microsoft Excel and Microcal Orgin Pro 8G software program (Microcal Software Inc., USA). An exponential curve fitting is performed on the corrected decay curve with the zero line (Fig. 4). The air exchange rate corresponds to (α) is calculated for every second. The frequency recorded by the instrument is plotted on the vertical axis, and it is proportional to the change in SF6 concentrations. The air volume flow ($\dot{v}$) can be calculated by multiplying the air exchange rate with the barn volume (V).

Experimental set-up for adsorption and resuspension measurements

Characterization of the wind tunnel

Resuspension and adsorption transmission parameters were investigated in a wind tunnel (Fig. 5) located at the Institute of Agricultural Engineering, University of Bonn. The wind tunnel features a square cross-section measuring 9.8 m in length and 0.9 m in width. At a distance of 5.4 m, a chipboard test platform (measuring 0.5 m × 1.2 m) was placed, which serves as the foundation for the built-in measurement technology. This technology includes two aerosol spectrometers, a temperature and humidity sensor, and two vane anemometers. The measured data are transmitted online and displayed graphically. Continuous monitoring during individual test series was facilitated through a Plexiglas viewing window.

Four axial ventilators (Ziehl-Abegg Company in Germany), each with a 0.3-m diameter, were installed. These ventilators allow adjustable air volume flow. To enhance air velocity at the channel bottom, a flapper plate with a 22-degree slope was positioned at the inlet. Transient flow occurs in the wind tunnel, while turbulent flow was observed during running measurements on the test platform, surpassing the critical Reynolds number limit (Re > 2320).

Measurement automation and control were achieved using LabView 8.5 software. This versatile software accommodates both adsorption and resuspension measurements. Climate parameters were graphically displayed at 2-s intervals, while aerosol spectrometer data were collected every second. Additionally, particle number concentration was classified into eight size classes based on

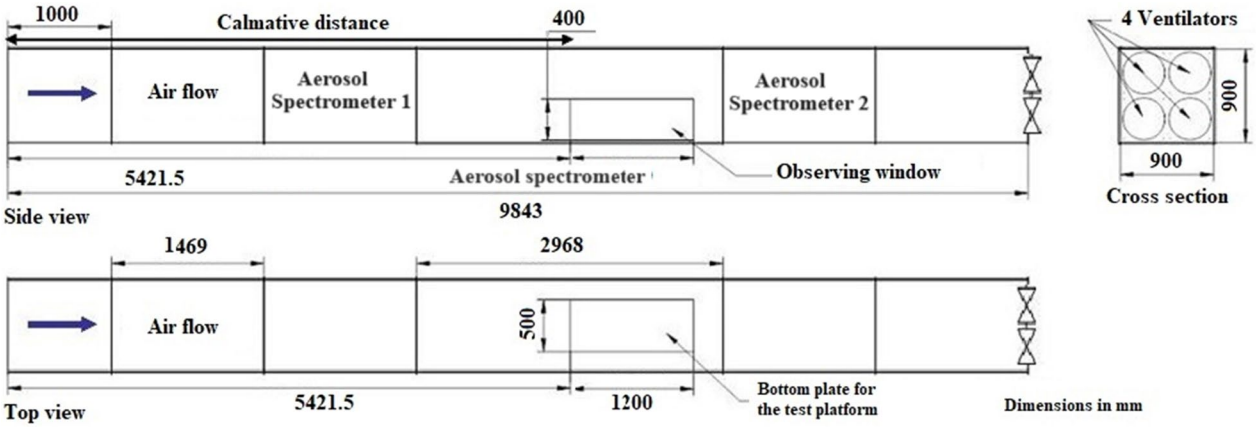

Fig. 5 The developed wind tunnel

optical equivalent diameter, ranging from 2.0 to > 20.0 microns.

Resuspension measurements

Resuspension measurements were conducted on a uniformly dry wooden plate (0.5 m × 1.2 m) located in the wind tunnel. The study examined three different air velocities: 2.1, 3.2, and 3.9 m s^{-1}. For consistency, a constant amount of dust collected from a dairy cattle barn (1.0 g) was used in the experiments.

The radially symmetrical intake heads of the aerosol spectrometers were precisely installed at the center of the platform. These heads were positioned at a horizontal distance of 0.1 m from each edge. Consequently, the distance between the two aerosol spectrometers was 1.0 m. All measuring instruments were placed 0.01 m above the wooden plate. Additionally, two vane anemometers (manufactured by Ahlborn Mess- und Regeltechnik GmbH, Germany) were diagonally positioned in the corners of the base plate. The study maintained a constant air velocity within the test platform area, and air temperature and humidity sensors were strategically placed in the platform corner.

The collected dust from the dairy cattle barn was positioned 0.1 m away from spectrometer II. It was then evenly distributed over a rectangular area measuring 0.005 m^2 (0.1 m × 0.05 m). Each resuspension measurement lasted 15 min, and nine replicates were conducted for each of the three investigated air velocities.

Spectrometer I records background concentration, while Spectrometer II detects resuspended particles. The resuspended particle mass is then calculated based on the previously determined particle size-specific density. The proportion of resuspended particulate mass is derived by the ratio of initial concentration and resuspended particles. The resuspension rate (Λ) as defined by Kim et al., [11], is the quotient of the mass flow of the resuspended particles (m_r°) and the initial mass on the surface (m_0) as expressed in Eq. 1:

$$\Lambda = m_r^{\circ} / m_0 \tag{1}$$

Resuspension rate (s^{-1}) is an indicator of how high the resuspended proportion of the particle mass as a function of the measurement duration and the initial concentration.

The resuspension factor (K_r) is defined by Schmidt and Nitschke [23] as the ratio of the particle concentration in the gas and the loading on the surface. The resuspension factor (m^{-1}) includes the resuspended particulate mass (g m^{-3}) for the specified 15-min measurement period and the initial 0.005 m^2 surface loading area (g m^{-2}). Both Λ and K_r were calculated for the eight size classes from 2.0 to > 20.0 µm.

Adsorption measurements

Wind tunnel adsorption measurements focused on particle adhesion to agricultural surfaces. To achieve this, a dispersing unit ensured continuous dust injection. Winter wheat (variety: Isengrain) at the early growth stage (EC 23—leaf area index of 1.25) served as the model plant due to its abundance near barns.

The dispersing unit, driven by a motor at a constant speed of 1200 RPM, continuously discharged 2.0 g of cattle dust over the platform. The injection height was 0.05 m above the platform surface, with 0.2 MPa pressure and 0.05 L per hour air volume flow.

A seed tray (0.50 m × 0.30 m) planted with wheat was positioned in the middle of the 1.20 m × 0.50 m test platform within the wind tunnel. Series measurements were conducted over 30 min at different air speeds: 2.8, 3.3, and 4.1 m s^{-1}.

Additionally, radially symmetrical intake heads of the aerosol spectrometers were installed 0.1 m away from the middle of the wheat tray on both sides. These spectrometers allowed measurement of particle number concentration. Aerosol Spectrometer I detected background concentration (installed before the wheat tray), while Aerosol Spectrometer II was placed after the wheat tray. Air velocity was measured using two vane anemometers located diagonally in the corners of the plate, and climate data (temperature and humidity) were recorded. Data transmission followed a similar approach as resuspension measurements. Wheat sampling occurred under both dry and moist conditions, with moistening achieved by spraying the plants with 50.0 ml of water. Particle number concentrations were measured before and after the adsorption surface, with the difference attributed to adsorption by the leaf surfaces. Using particle size-specific density, the adsorbed particle mass of the wheat was calculated.

Results and discussion

Analysis of the cattle dust

Describing and analyzing PM collected from dairy cow barns helps identify its sources and narrow down dust origins for potential reduction.

Weende analysis

Weende analysis is suitable for the classification of organic and inorganic matter. The results of the Weende analysis with regard to the cattle dust collected from the barn showed that 90.2% of the investigated dust was dry matter (902 g kg^{-1}). Dry matter (DM) is composed of organic and inorganic substances. 38.0% of DM content was crude protein (307 g kg^{-1} DM) and 36.0% was crude ash (287 g kg^{-1} DM). The crude ash contains inorganic constituents.

The presence of crude protein and ash indicates that the dust may contain animal feed and manure. The crude fiber content (57 g kg^{-1} DM) represented 7.0% of DM and is attributed to cellulose and lignin. The nitrogen-free extractive (156.5 g kg^{-1} DM) with 19% from DM consists of easily soluble substances such as sugar and starch. The analysis of the trace and bulk elements showed the highest proportion of calcium at 16.2 g kg^{-1} DM and then followed by potassium with about 9.6 g kg-1 DM. The high levels of calcium and potassium suggest that the dust may be derived from animal feed or bedding materials. Phosphorus (5.8 g kg^{-1} DM) and magnesium (4.6 g kg^{-1} DM) were almost equal while the amount of sodium was 2.1 g kg^{-1} DM. The presence of phosphorus and magnesium may also indicate the presence of manure. These results provide valuable information for identifying the origin of the dust in the dairy barn which matches with the study contacted by [2] on poultry and pig barns.

C:N ratio

C:N ratio analysis was conducted using two dust samples, S1 and S2. As illustrated in Fig. 6, the average values for nitrogen (N) and carbon (C) contents were 4.4, 34.5% and 5.3, 38.4% for S1 and S2, respectively. Accordingly, C:N was 7.84:1 for S1 and 7.25:1 for S2. As presented by C:N ratio, the majority of cattle dust consists of carbon fraction which is one of the main ingredients for litter and feed. The small proportion of nitrogen probably refers to the excretions and skin or hair particles of the animals. Therefore, it can be concluded that the cattle dust mostly comes more from the provided services to the animals than from the animals themselves.

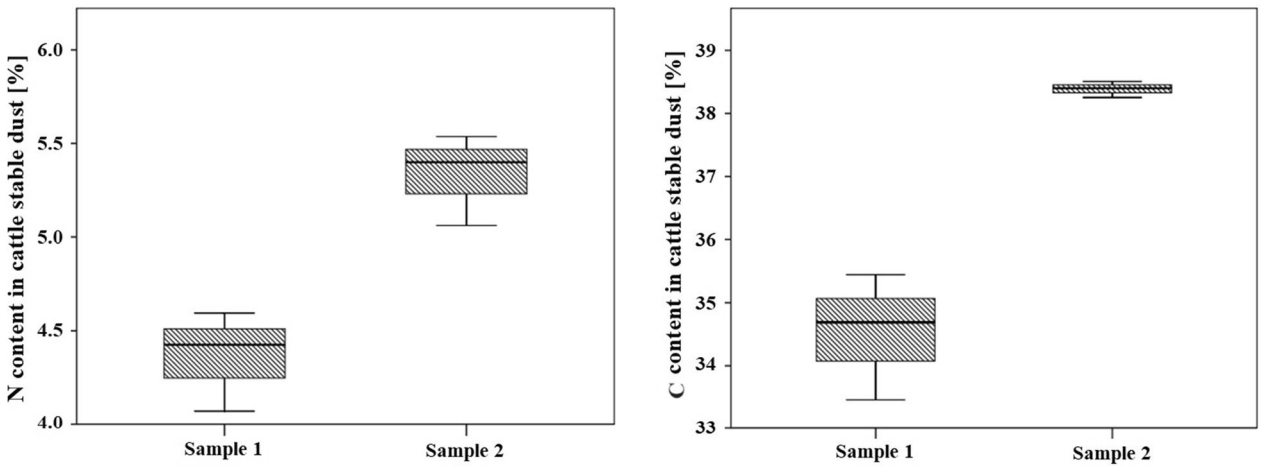

Fig. 6 C:N analysis of the collected dust from dairy barn

Dust emission from investigated dairy cows barn

Particle mass concentration was calculated from measured particle number concentration, allowing estimation of dust emissions from the dairy cow barn based on ventilation rate and particle mass concentration within the barn.

Estimation of the particle mass concentration

To calculate the mass concentration of particles, it is essential to determine both the particle size-specific shape factor and density. Microscopic analysis on dairy cattle dust samples was conducted, specifically examining the variety of particle shapes across different size classes (Fig. 7). This microscopic analysis serves as the foundational basis for calculating the particle shape factor.

The particle shape factor provides information about the geometry of individual particle size classes. A shape factor of 1.0 corresponds to a sphere. The larger the deviation from 1.0, the more polymorphous the shape appears. Descriptive statistics for the particle size-specific shape factors are listed in Table 1.

The particle shape factor increases with increasing the size fraction due to the possibility of a wide variety of different shapes with increasing the particles size. The shape factor was increased slightly for the particle size above 7.5 µm to reach approximately 1.67 µm for a particle size > 20.0 µm as illustrated in Table 1.

The density of examined dairy cow dust in relation to the particle's diameter is shown in Fig. 8. Higher density was observed with small particles' diameter (from 4 to 7 µm). The density of 2.742 kg m^{-3} for the smallest particles' diameter (4.0–≤5.0 µm) may be returned to the mineral constituents of the particles. An inverse relationship was observed between both particles' diameter and the density of examined particles from a cattle barn. Increasing of particles diameter leads to a decrease in particles density. Thus, the density was 784 kg m^{-3} with a particle size of 15.0– ≤20.0 µm. However, the density increases again at a particle size of > 20.0 µm to reach 1198 kg m^{-3}. Slight increase in particles density for particles > 20.0 µm can be explained by the microscopic analysis where the agglomerations occurred. The smaller mineral particles presumably adhere to the larger particles and could thus influence the density of the agglomerated particles at diameter > 20.0 µm.

From estimated particles density and particles mass factor [µg], consequently the particles mass concentration [µg m^{-3}] was calculated for each particle size class based on the measured particle number concentration [particle m^{-3}]. Figure 9 illustrates the particle number and mass concentrations within the barn during the winter season. The smallest particles size classes (up to 1.0–≤1.6 µm) represented approx. 96.1% of the total

Table 1 Particle size-specific dimensionless shape factors for the investigated dairy cows dust

Size fraction (µm)	Shape factor (κ) (mean ± standard deviation)	Variance	Standard error
> 2.0–≤ 3.0	1.09 ± 0.09	0.06	0.05
3.0–≤ 4.0	1.06 ± 0.05	0.05	0.02
4.0–≤ 5.0	1.06 ± 0.05	0.02	0.01
5.0–≤ 7.5	1.10 ± 0.09	0.06	0.01
7.5–≤ 10.0	1.17 ± 0.15	0.06	0.01
10.0–≤ 15.0	1.25 ± 0.23	0.05	0.01
15.0–≤ 20.0	1.40 ± 0.31	0.40	0.04
> 20.0	1.67 ± 0.42	0.28	0.02

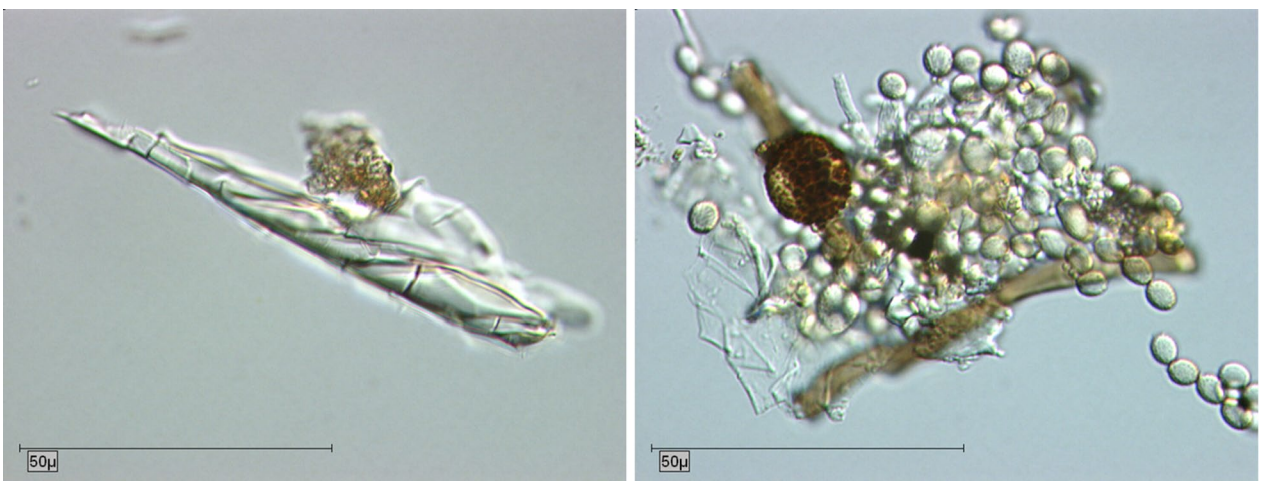

Fig. 7 Microscopic images of agglomerated particles

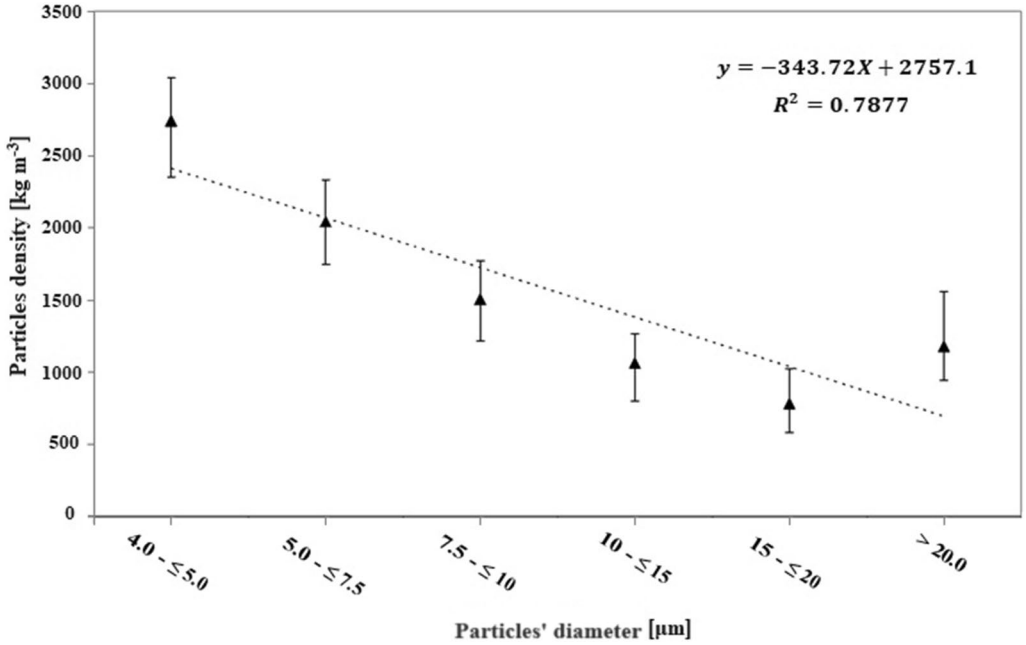

Fig. 8 Size-specific density for collected particles dairy cows' barn

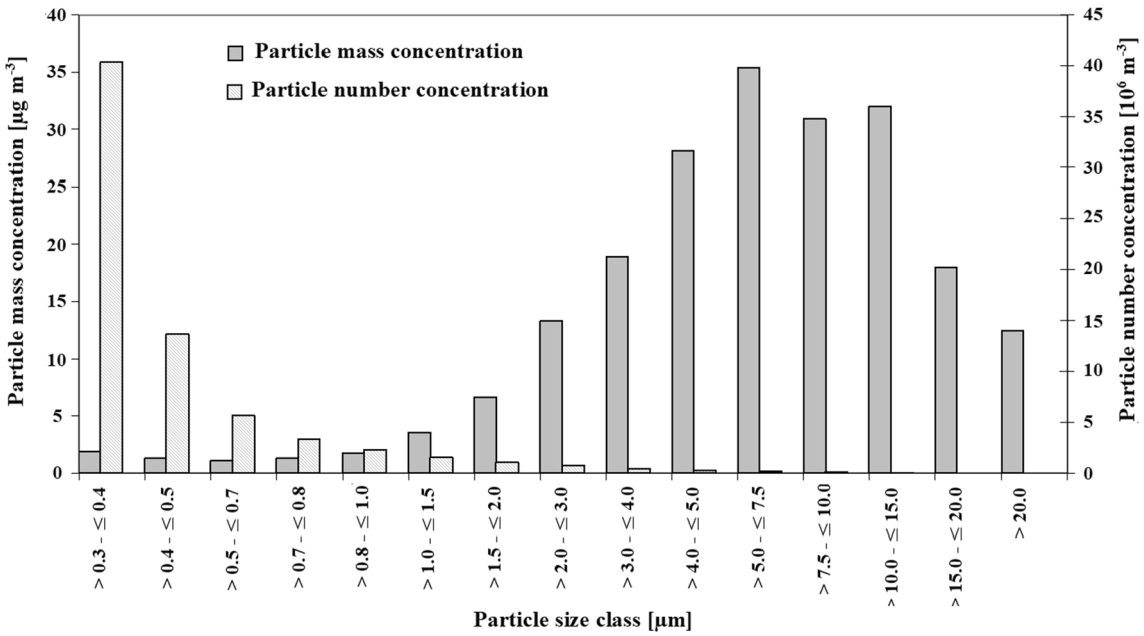

Fig. 9 Particle number and mass distribution for the examined barn under winter conditions

particle number concentration with small proportion of the particle mass concentration around 5.2%. Maximum particle mass concentration of approx. 35.3 µg m^{-3} was observed with particle size class of 5.0–≤7.5 µm.

The distribution of particles mass for $PM_{2.5}$, PM_{10}, and PM_{total} throughout the day emphasized the role of main activities such as litter spreading and milking on concentration (Fig. 10). Similar trends were observed with other measuring days as well. Differences were identified between the individual fractions as expected with particularly evident in the strong peaks at afternoon hours. The average of particle mass concentrations was

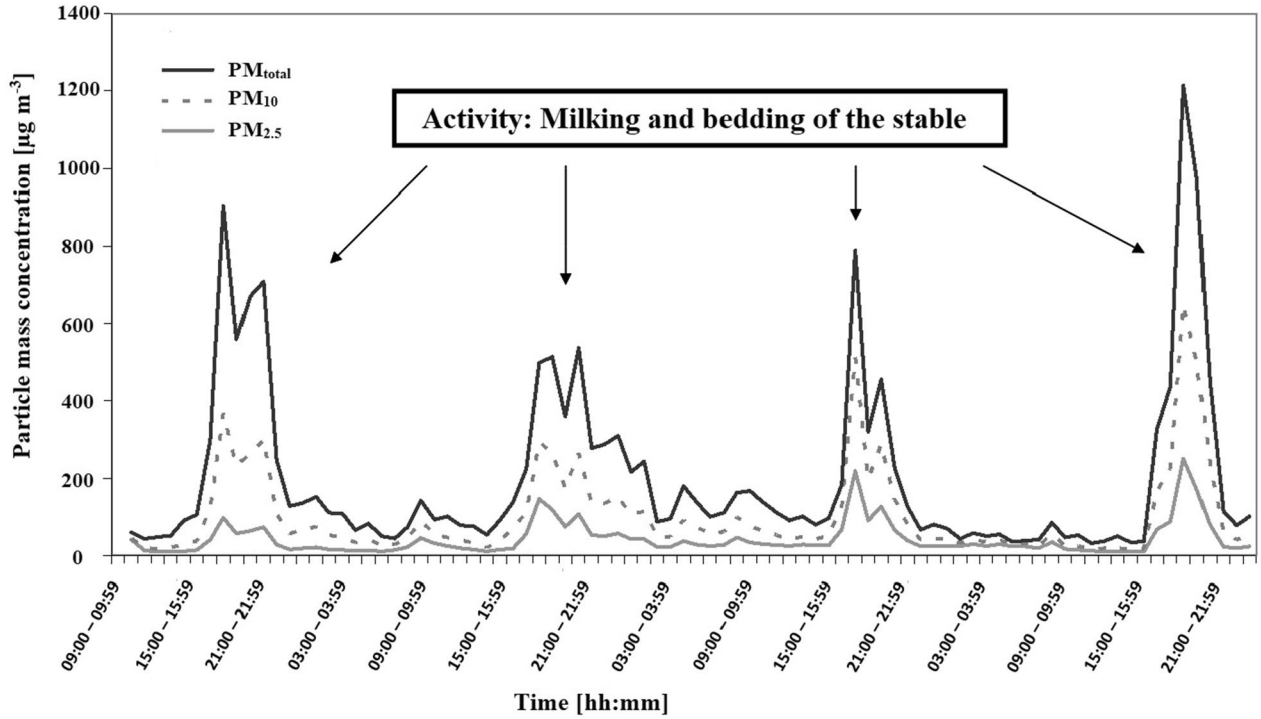

Fig. 10 Daily profiles of the particle mass concentration in the studied barn under transitional conditions

39.1, 94.6, and 184.9 µg m^{-3} for $PM_{2.5}$, PM_{10}, and PM_{total}, respectively.

Ventilation rate

The air volume flow ($\dot{v}$) in the eaves–ridge ventilated cattle barn was determined via tracer gas decay method using SF6. A close correlation between air volume flow and wind speed (v_w) outside the barn has been found as shown in Fig. 11. The air volume flows recorded in the barn were found to be similar throughout the entire experimental period. A low volume flow was observed at night and early morning hours and increased with increasing the wind speed. The average daily wind speed was 0.8 m s^{-1} while the air volume flow was 23030 m^3 h^{-1}.

The main wind direction was until about 8:00 am from the south-east. After that, there were fluctuations from the south, south-west, and south-east directions. At 6:00 pm, the wind blew constantly from the south. The average outside and inside temperatures were 17.7 and 19.2 ℃, respectively, and the average relative humidity was 67.1%.

The coefficient of determination (R^2) represents the relationship between the parameters air volume flow and wind speed as a function of the wind direction. R^2-values were 0.509 ($n=77$), 0.498 ($n=64$), and 0.203 ($n=58$) for summer, winter, and transition season, respectively.

A positive relationship between air volume flow and wind speed ($R^2=0.6105$, $n=40$) as results for the main wind direction south-east for summer measurements was observed (Fig. 12). The maximum wind speed was 2.9 m s^{-1}. During the transition measurement, no unique main wind direction was assigned where the wind blew from south, south-west, and west. The coefficient of determination for south-west was $R^2=0.207$ ($n=21$). The wind blew during the winter measurement mainly from the south with $R^2=0.535$ ($n=30$).

The descriptive statistics of the air volume flow at the different seasons are illustrated in Table 2. The average annual air volume flow was approx. 27.198 m^3 h^{-1} with more fluctuation occurred during the summer season. The lowest wind speeds were recorded during the summer measurement at 1.0 m s^{-1}. The mean wind speed differs only by 0.1 m s^{-1} during the transition and winter. The wind directions (Φ_W) were in average from south-east in summer, south-west in transition, and south in winter.

The results of the regression analysis, which examined the relationship between the air volume flow and the dependent variable based on measurements taken during different seasons, are shown in Table 3. The inclusion of the climate parameters indoor temperature (T_i) and relative humidity (RH) in the model lead to a slight improvement in the calculation of the air volume flow

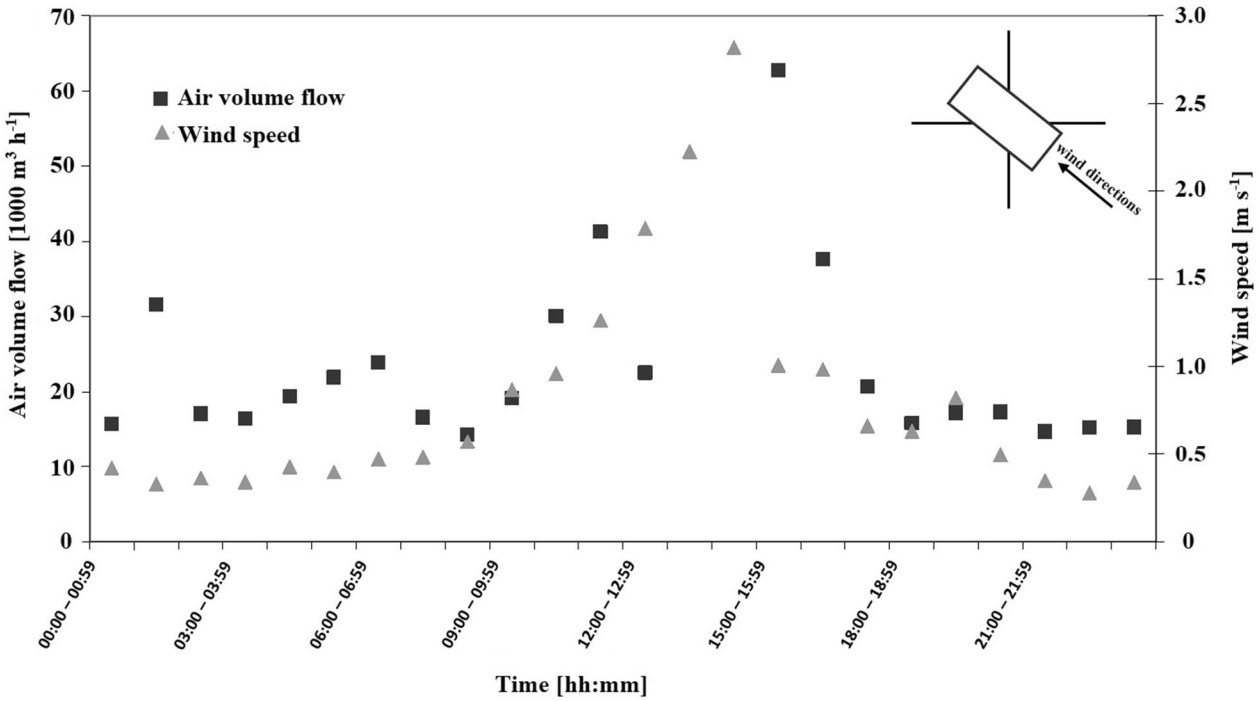

Fig. 11 Daily air volume flow and wind speed for the investigated barn under summer conditions

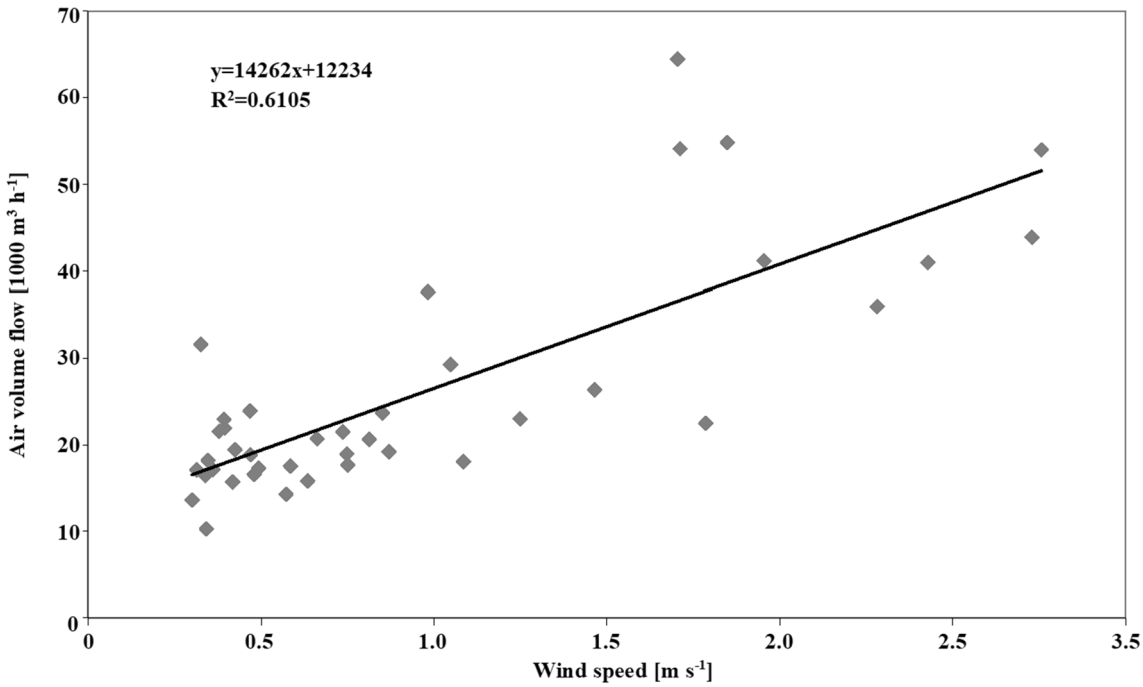

Fig. 12 Relationship between air volume flow and wind speed in the main wind direction south-east under summer conditions in the investigated barn

Table 2 Air volume flow and meteorological parameters determined in seasonal dependence for the examined barn

Year season	$\dot{v}$ [$m^3\ h^{-1}$]	vw [$m\ s^{-1}$]	Φ_W	Ta [°C]	Ti [°C]
Summer	26268.90 ± 15353.86	1.01 ± 0.67	South-East	16.71	18.31
Transition	28060.99 ± 9799.07	1.41 ± 0.62	South-west	9.98	11.99
Winter	27266.35 ± 8172.65	1.51 ± 0.55	South	9.46	10.14

in summer season. The regression model for the summer measurement is shown in Eq. 2. The wind speed has the highest influence on this regression model while the relative humidity is negatively correlated. The relative humidity during the transition measurements had the highest influence on the regression model (Eq. 3). The wind speed had low influence on the calculation of the air volume flow while T_i, RH, and Φ_W had a negative correlation with respect to the air volume flow. The regression model for winter measurements is explained in Eq. 4. RH and v_w had a very high influence on air volume flow while Φ_W was negatively correlated:

$$\dot{v} = 40,115.85 + 933.39Ti - 280.13RH + 13,198.64vw - 1,686.15Ta + 22.56\Phi W \quad (2)$$

$$\dot{v} = 78,041.99 - 5,244.22Ti - 321.83RH + 77.14vw + 4.809.88Ta - 46.49\Phi W \quad (3)$$

$$\dot{v} = 113,881.84 - 3,339.88Ti - 693.01RH + 6,298.87vw - 350.85Ta + 1.65\Phi W \quad (4)$$

The average air exchange rates (AER) for the investigated barn were 41.8, 48.5, and 55.6 h^{-1} for summer, transition, and winter seasons, respectively. As observed, AER was lower in summer compared to winter and transition seasons. The possible explanations for this unexpected result may return to the limited eaves–ridge ventilation system in the barn in addition to the interplay of weather and animal behavior. In high air temperature, the cattle may reduce overall movement. Less active cattle contribute to a lower AER during summer.

Dust emission from the examined barn was calculated based on particle mass concentrations and ventilation rates. Additionally, the seasonal effect on dust emission was estimated. Notably, higher dust emission occurred during the transition season due to the combination of elevated particle mass concentration and air volume flow (Fig. 13). The mean particle mass concentration was 0.206 mg m^{-3} for summer, 0.198 mg m^{-3} for transition, and 0.140 mg m^{-3} for winter season.

Interestingly, measurements taken during transition season exhibited greater scattering of PM compared to the other seasons. Overall, dust emissions in the dairy cattle barn were 0.086 g h^{-1} LU^{-1}, 0.11 g h^{-1} LU^{-1}, and 0.068 g h^{-1} LU^{-1} for summer, transition, and winter, respectively. Importantly, these emissions remain below the prescribed values in Germany. According to [15], dust emissions in exhaust air must not exceed 0.2 kg h^{-1} of mass flow.

Transmission parameters of particles from cattle barn

Particle size-specific resuspension

The resuspension measurements of 15 min were conducted in a wind tunnel using 0.1 g dairy cattle dust for each measurement (Fig. 14). Resuspended particulate mass is performed as PM_{total} and the average wind speed was 3.2 m s^{-1}. Different peaks occurred during a resuspension measurement, however no continuous resuspension was detected. The first peak showed the highest resuspended particle mass of approximately 8.8 mg m^{-3} at the beginning of the measuring period till the fans reach to the set wind speed. Middle peaks showed scattered resuspended particle masses of 2.5–5.0 mg m^{-3}. Minor resuspensions reached below 1.0 mg m^{-3}. Accordingly, very small amounts of the dust resuspend and only occasionally pass larger amounts as peaks into the air flow.

Table 3 Regression analysis for the air volume flow as a dependent variable based on different seasons measurements data

Parameter	Summer			Transition			Winter		
	Regression coefficient	r	Significance	Regression coefficient	r	Significance	Regression coefficient	r	Significance
T_i	933.39	0.390	0.620	− 5244.22	0.259	0.063	− 3339.88	− 0.008	0.017
RH	− 280.13	− 0.499	0.130	− 321.83	− 0.530	0.002	− 693.01	− 0.729	0.000
v_w	13,198.64	0.631	0.000	77.14	0.427	0.979	6298.87	0.712	0.007
T_a	− 1686.15	0.304	0.272	4809.88	0.338	0.082	− 350.85	0.588	0.847
Φ_W	22.56	0.158	0.600	− 46.49	− 0.262	0.061	1.65	− 0.146	0.925

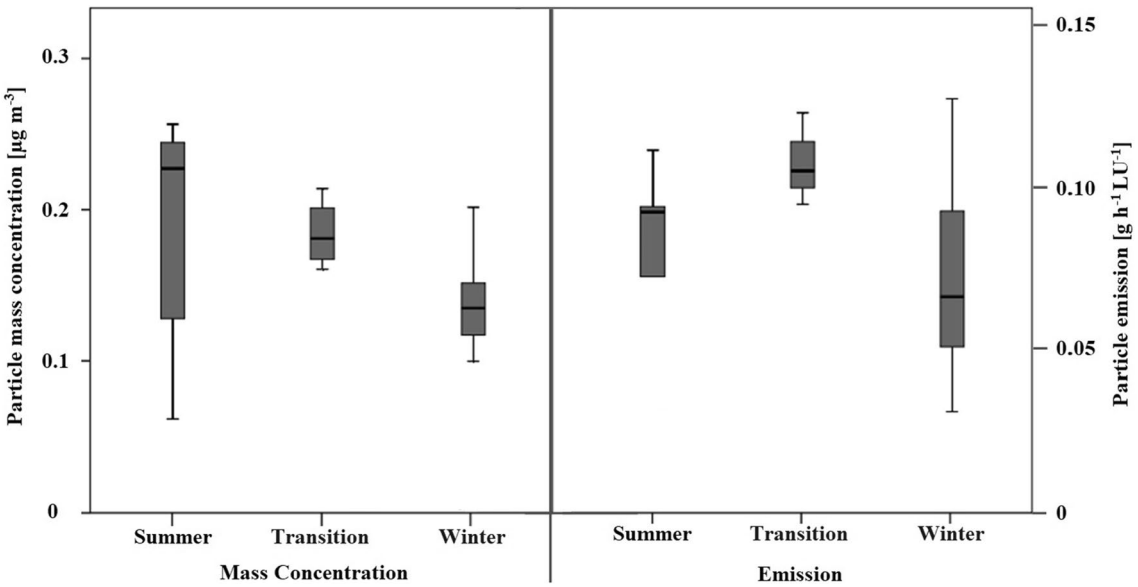

Fig. 13 Comparison of the particle mass concentration and emission as a function of the year seasons

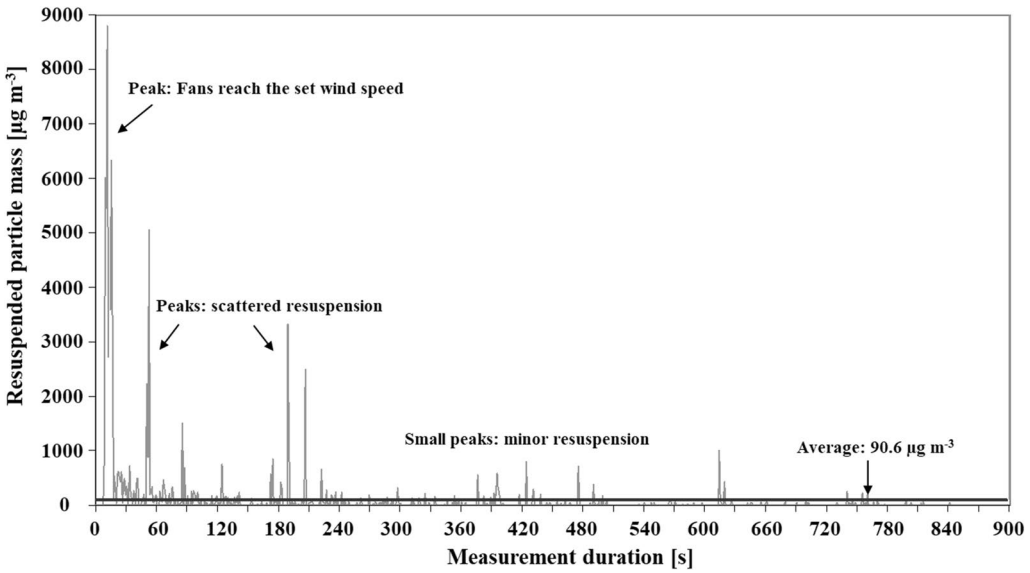

Fig. 14 Resuspension behavior of PM_{total} from cattle barn at 3.2 m s^{-1} wind speed in the wind tunnel

The resuspended mass concentration depending on the particle size fraction and wind speed in the wind tunnel is illustrated in Fig. 15. A similar justification proposed by [20] and [18], the proportion of resuspended particles mass increases exponentially with increasing particle size class. The mean resuspended particle mass concentrations for the particle size class 15.0–≤20.0 µm was 2.8, 12.9, and 7.5 mg m^{-3} at 2.1, 3.2, and 3.9 m s^{-1} wind speed, respectively. The highest resuspended particles mass concentration is achieved at a wind speed of 3.2 m s^{-1}. It is possible that the decrease in resuspended particle mass concentration at 3.9 m s^{-1} is due to the saturation effect. This occurs when the wind speed is high enough to lift all the available particles from the injection source, after which further increases in wind speed do not lead to an increase in particle resuspension.

As expected, the resuspension rate (Λ) and the resuspension factor (k) are very low for the investigated dairy cattle dust. Similar to the resuspended particle mass, both Λ and k were increased with increasing the

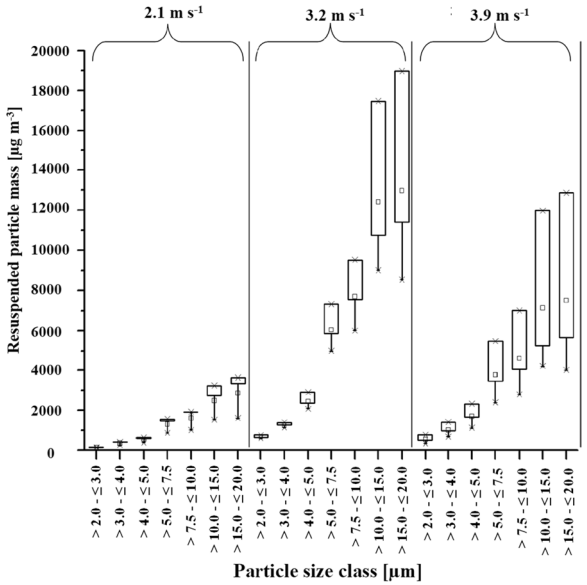

Fig. 15 Resuspended particle mass concentration of 0.1 g cattle dust with respect to different wind speeds in the wind tunnel

wind speed and particle size class as presented by [18]. The average resuspension rates ranged between 0.00004 and 0.00034 s^{-1} while the resuspension factors averaged between 0.029 and 0.133 m^{-1} depending on the wind speed.

From the above results, there is neither a continuous resuspension of the particles nor a complete removal of the particle layer over the entire measurement period of 15 min. On the contrary, individual particles detach from the discharged layer of dust at indefinite times and enter the air flow, resulting in isolated resuspension peaks.

Furthermore, as observed more particles can be resuspended in the initial phase. Towards the end of the measurement, the resuspended particle mass falls to the level lower of the mean value where the estimated error is 25%. The resuspension rate decreases as a function of time and increases with increasing wind speed and the particle size. This result is confirmed by [18] which describes resuspension tests in a wind tunnel with grass as the surface.

Particle size-specific adsorption

The adsorbed particulate mass is expressed as $PM_{ad\text{-}total}$. A plant stand is continually influenced by external factors due to its structure. In addition to gravity, wind speed as presented by [21] plays a significant role in the adsorption rate. As wind currents strengthen, pronounced leaf movement occurs, resulting in a dynamically changing leaf surface. Consequently, particles have the opportunity to pass through the leaves due to the flow. Interestingly, despite their small proportion, particles captured by the wheat exhibit unexpectedly robust adsorption as the size class increases. As He et al. [8] explained, leaf structure plays a crucial role in determining the ability to retain PM of varying sizes. It is worth noting that leaves with a wax layer, such as those found in wheat, tend to accumulate predominantly larger PM particles.

A plant stand, being a non-rigid system with a changeable shape, exhibits fluctuating adsorption rates (Fig. 16). In this context, the mean value of the adsorbed particle mass was 20.19 µg m^{-3}. Notably, the highest peak occurred at an adsorbed particle mass of 991.2 µg m^{-3}. Throughout the entire measurement period, significant fluctuations in the adsorbed particle mass were evident, emphasizing the absence of a continuous adsorption rate.

The adsorbed particle mass concentration of wheat at an air speed of 2.8 m s^{-1} is depicted in Fig. 17. To assess particle behavior, a mass balance measurement was conducted, comparing particle concentrations in front of and behind the wheat crop. Notably, the adsorption rate increased with larger particle size fractions, as shown in Fig. 17. Across all size fractions, the adsorbed particle mass concentration averaged 20.9 mg m^{-3}, resulting in an overall adsorption rate of approximately 74.9%.

The adsorption rates of wheat in relation to particle size fractions and air speeds are illustrated in Fig. 18. The adsorption rates for wheat at three air speeds exhibit a strong linear relationship. This is supported by a high coefficient of determination (Fig. 18). This finding implies that as particle size increases, wheat's adsorption capacity also rises proportionally. Remarkably, the wheat's adsorption capacity is most pronounced at air speeds below 4.1 m s^{-1}. At an air speed of 3.3 m s^{-1}, the wheat achieves its highest adsorption rate across nearly all size fractions. The observed phenomenon can be attributed to the optimal interaction between the wheat leaf surface and airborne particles at moderate air speeds, enhancing adsorption efficiency. Additionally, these moderate air speeds may promote particle agglomeration, leading to even more efficient adsorption processes. Particularly noteworthy is the particle size fraction of > 15.0–≤ 20.0 µm, which demonstrates an impressive adsorption rate of almost 90.0%.

Conclusion

The recent study not only examines dust emissions from cattle barns, but also sheds light on the complex process of fine dust transmission. By meticulously characterizing particle matter, assessing aerodynamic properties, and

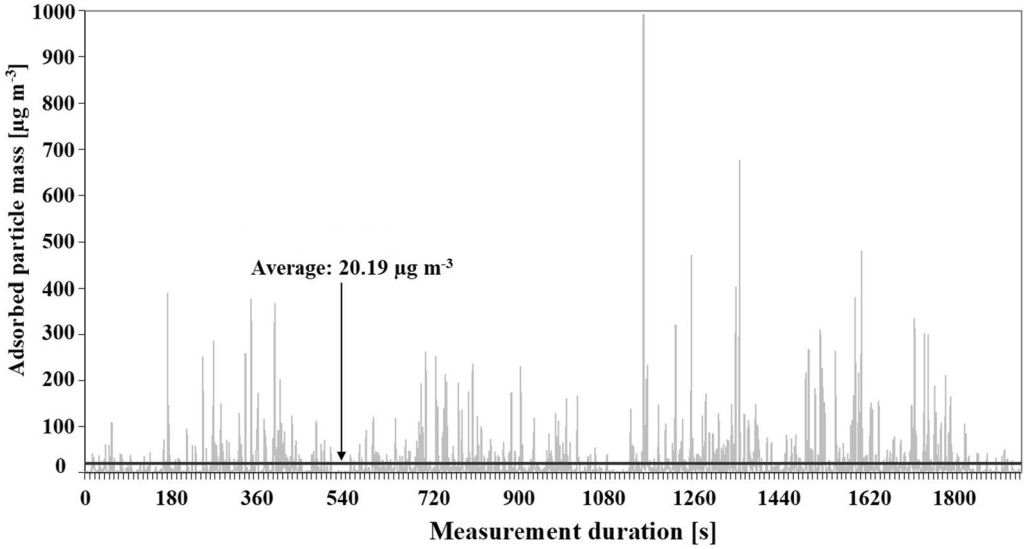

Fig. 16 Adsorption behavior of wheat at early growth stage of EC 23 and average wind speed of 3.3 m s^{-1} in the wind tunnel for PM_{total}

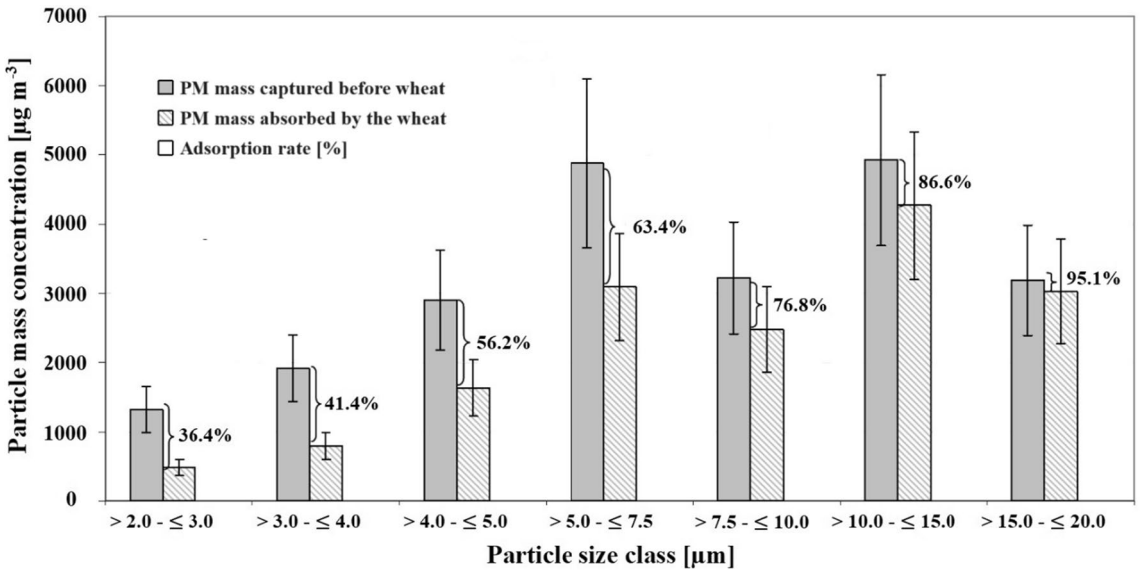

Fig. 17 Adsorption measurement with dry wheat (EC 23) at an average wind speed of 2.8 m s^{-1} in the wind tunnel over 30 min measurement duration

measuring dust emissions, a robust data package for precise propagation simulations and predictive models were provided.

Long-term measurements within the examined barn allowed to discern seasonal variations in particle mass concentrations. Additionally, using the tracer gas decay method, the ventilation rates were accurately estimated and thus the particle emission rates.

Initial insights into fine dust transmission—specifically through resuspension and adsorption parameters—underscore their important role. However, further research is imperative for reliable dispersion model predictions. Notably, both resuspension rate and factor remain low, despite minimal aerogenic resuspension due to wind.

Winter wheat, as evidenced by the adsorption measurements, exhibits a commendable adsorption rate. Nevertheless, opportunities for expansion exist. The investigation of adhesion abilities among diverse plant types surrounding animal barns is recommended. By

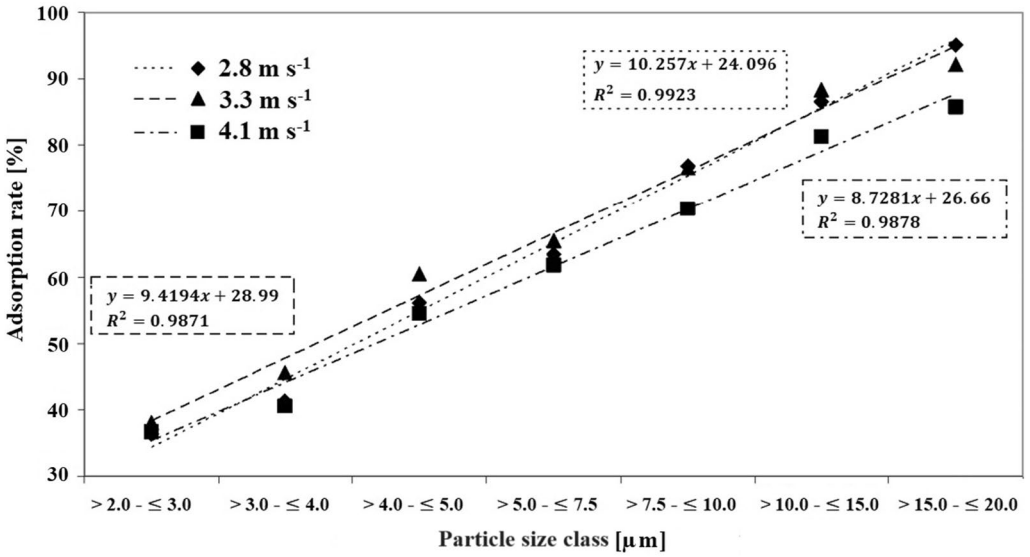

Fig. 18 Particle size-specific adsorption rates of dry wheat (EC 23) at different wind speeds in the wind tunnel over 30 min measurement duration

incorporating a variety of plant materials, precise insights into the adsorption capacities of specific vegetation types per square meter can be obtained. This research avenue offers potential for optimizing barn environments, improving air quality, and advancing sustainable practices.

Acknowledgements
The authors extend their sincere appreciation to all the diligent laborers in the dairy cattle barns, whose unwavering efforts were instrumental in the successful execution of our research. Additionally, we would like to acknowledge the STDF/EKB organization, which generously supports open access publication by covering the article fees.

Author contributions
EM suggested the conceptual of the research methodology, writing—review and editing the original draft. JP implemented the research methodology and data curation. HRSA wrote and prepared the original draft. WB suggested the overall conceptual of the research and supervised the whole process in addition to management and acquisition of the funding.

Funding
Open Access funding enabled and organized by Projekt DEAL. This study was funded by German Research foundation (DFG—Deutsche Forschungsgemeinschaft).

Availability of data and materials
All data generated or analyzed during this study are included in this published article.

Declarations

Ethics approval and consent to participate
Not applicable.

Consent for publication
Not applicable.

Competing interests
The authors declare that they have no competing interests.

Received: 5 October 2023 Accepted: 16 January 2024
Published online: 27 February 2024

References

1. Beer CG, Hendricks J, Righi M, Heinold B, Tegen I, Groß S, Sauer D, Walser A, Weinzierl B (2020) Modelling mineral dust emissions and atmospheric dispersion with MADE3 in EMAC v254. Geosci Model Dev 13(9):4287–4303. https://doi.org/10.5194/gmd-13-4287-2020
2. Cambra-López M, Hermosilla T, Aarnink AJA, Ogink NWM (2012) A methodology to select particle morpho-chemical characteristics to use in source apportionment of particulate matter from livestock houses. Comput Electron Agric 81:14–23. https://doi.org/10.1016/j.compag.2011.11.002
3. Chaurasia M, Patel K, Tripathi I, Rao KS (2022) Impact of dust accumulation on the physiological functioning of selected herbaceous plants of Delhi, India. Environ Sci Pollut Res 29(8):80739–80754. https://doi.org/10.1007/s11356-022-21484-4
4. Chmielowiec-Korzeniowska A, Trawińska B, Tymczyna L, Bis-Wencel H, Matuszewski Ł (2021) Microbial contamination of the air in livestock buildings as a threat to human and animal health—a review. Ann Anim Sci 21(2):417–431. https://doi.org/10.2478/aoas-2020-0080
5. Elfman L, Wålinder R, Riihimäki M, Pringle J (2011) Air Quality in Horse Stables. In N. Mazzeo (Ed.), Chemistry, Emission Control, Radioactive Pollution and Indoor Air Quality (pp. 3–24). IntechOpen. https://doi.org/10.5772/18228
6. Ferro AR (2022) Resuspension. In: Zhang Y, Hopke PK, Mandin C (eds) Handbook of indoor air quality. Springer, Singapore, pp 14–23. https://doi.org/10.1007/978-981-10-5155-5_11-1
7. Guo L, Zhao B, Jia Y, He F, Chen W (2022) Mitigation strategies of air pollutants for mechanical ventilated livestock and poultry housing—A review. Atmosphere 13(3):452. https://doi.org/10.3390/atmos13030452
8. He L, Wang S, Liu M, Chen Z, Xu J, Dong Y (2023) Transport and transformation of atmospheric metals in ecosystems: a review. J Hazardous Mater Adv 9:100218. https://doi.org/10.1016/j.hazadv.2022.100218
9. Henseler J, Rosenthal E, Lodomez P, Nannen C, Diekmann B, Büscher W (2009) Resuspension of dust from livestock buildings: influences and fluctuation factors. Landbauforschung Völkenrode 59(3):198–201
10. Kim KH, Kabir E, Jahan SA (2018) Airborne bioaerosols and their impact on human health. J Environ Sci 67:23–35. https://doi.org/10.1016/j.jes.2017.08.027

11. Kim Y, Gidwani A, Wyslouzil BE, Sohn CW (2010) Source term models for fine particle resuspension from indoor surfaces. Build Environ 45(8):1854–18651. https://doi.org/10.1016/j.buildenv.2010.02.016
12. Li L, Yang J, Zhou Q, Peijnenburg WJGM, Luo Y (2020) Uptake of microplastics and their effects on plants. In: Defu H, Yongming L (eds) Microplastics in terrestrial environments. The handbook of environmental chemistry, vol 95. Springer, Cham. https://doi.org/10.1007/698_2020_465
13. Linda J, Pospíšil J, Köbölová K (2023) Identification of wind-induced particle resuspension in urban environment using CFD modelling. Atmosphere. https://doi.org/10.3390/atmos14010057
14. Mostafa E, Buescher W (2011) Indoor air quality improvement from particle matters for laying hen poultry houses. Biosys Eng 109:22–36. https://doi.org/10.1016/j.biosystemseng.2011.01.011
15. Mostafa E, Diekmann B, Buescher W, Schneider T (2016) Analysis of the dust emissions from a naturally ventilated turkey house using tracer gas method. Environ Monit Assess 188(7):377. https://doi.org/10.1007/s10661-016-5355-7
16. Mostafa E, Nannen C, Henseler J, Diekmann B, Gates RS, Buescher W (2016) Physical properties of particulate matter from animal houses—empirical studies to improve emission modelling. Environ Sci Pollut Res 23(12):12253–12263. https://doi.org/10.1007/s11356-016-6424-8
17. Naumann C, Bassler R (1988) Methodenbuch Band III. Die chemische Untersuchung von Futtermitteln. Verband Deutscher Landwirtschaftlicher Untersuchung- und Forschungsanstalten, Neumann-Neudamm, Melsungen.
18. Nicholson KW (1993) Wind tunnel experiments on the resuspension of particulate material. Atmos Environ A Gen Top 27(2):181–188. https://doi.org/10.1016/0960-1686(93)90349-4
19. Papanastasiou DK, Fidaros D, Bartzanas T, Kittas C (2011) Monitoring particulate matter levels and climate conditions in a Greek sheep and goat livestock building. Environ Monit Assess 183:285–296. https://doi.org/10.1007/s10661-011-1921-1
20. Qian J, Ferro AR (2008) Resuspension of dust particles in a chamber and associated environmental factors. Aerosol Sci Technol 42(7):566–5781. https://doi.org/10.1080/02786820802220274
21. Ram SS, Majumder S, Chaudhuri P, Chanda S, Santra SC, Chakraborty A, Sudarshan M (2015) A review on air pollution monitoring and management using plants with special reference to foliar dust adsorption and physiological stress responses. Crit Rev Environ Sci Technol 45(23):2489–2522. https://doi.org/10.1080/10643389.2015.1046775
22. Reznik G, Schmidt E (2008) Abscheidung von Feinstaub an Pflanzen bei niedrigen Strömungsgeschwindigkeiten. Chem Ing Tec 80(1):1849–1853
23. Schmidt E, Nitschke D (2006) Aufwirbelung von auf Oberflächen abgelagerten Partikelschichten. Chem Ing Tec 78(5):525–533
24. VDI (Verein Deutscher Ingenieure) (1999) Messen von Partikeln—Gravimetrische Bestimmung der Massenkonzentration on Partikeln in der Außenluft—Grundlagen (VDI-Richtlinie 2463, Blatt 1). Beuth Verlag. https://www.beuth.de/de/technische-regel/vdi-2463-blatt-1/104883
25. Yang X, Lee J, Barker DE, Wang X, Zhang Y (2012) Comparison of six particle size distribution models on the goodness-of-fit to particulate matter sampled from animal buildings. J Air Waste Manag Assoc 62(6):673–682. https://doi.org/10.1080/10962247.2012.671148

Publisher's Note